International Journal of Mass Spectrometry 303 (2011) 90–96

Contents lists available at ScienceDirect

International Journal of Mass Spectrometry

journal homepage: www.elsevier.com/locate/ijms

Structural elucidation of degradation products of olaquindox under stressed conditions by accurate mass measurements using electrospray ionization hybrid ion trap/time-of-flight mass spectrometry

Zhao-Ying Liu[a], Hua-Hai Zhang[b], Xiao-Jun Chen[a], Xiao-Ni Zhou[a], Leren Wan[c], Zhi-Liang Sun[a,*]

[a] Hunan Engineering Research Center of Veterinary Drugs, College of Veterinary Medicine, Hunan Agricultural University, Furong District, Changsha, Hunan 410128, China
[b] College of Forestry, Northwest Agriculture and Forestry University, Yangling, Shanxi 712100, China
[c] Shimadzu International Trading (Shanghai) Co., Limited, Shanghai 200052, China

ARTICLE INFO

Article history:
Received 7 December 2010
Received in revised form 1 January 2011
Accepted 7 January 2011
Available online 14 January 2011

Keywords:
Olaquindox
LC/MS-IT-TOF
Degradation product
Photo-degradation
Mass spectrometry

ABSTRACT

In this study, the stress degradation of olaquindox under conditions of hydrolysis (neutral, acidic and basic), oxidation and photolytic stress was investigated. In order to characterize each degradation product, we developed a rapid, sensitive and reliable high-performance liquid chromatography combined with hybrid ion trap/time-of-flight mass spectrometry (LC/MS-IT-TOF) method. The degradation products formed under different forced conditions were separated using an ODS-C18 column with gradient elution. Multiple scans of degradation products in MS and MS/MS modes and accurate mass measurements were performed through data-dependent acquisition. The structural elucidations of degradation products were performed by comparing the changes in the accurate molecular masses and fragment ions generated from precursor ions with those of parent drug. The present results showed that maximum degradation was observed in hydrolysis, especially in the acidic condition. The drug was also degraded significantly under photolytic conditions. A total of 12 degradation products of olaquindox were detected and characterized using the developed method. The main degradation product was formed by the complete cleavage of side chain to form 3-methyl-2-hydroxylquinoxaline-4-oxide. A degradation pathway of olaquindox was also tentatively proposed for the first time based on these characterized structures.

1. Introduction

The identification of drug degradation products plays an important role in the drug discovery and development processes. It has been well documented that drug products will undergo physicochemical degradation during manufacturing processes and storage [1]. Stress testing of the drug substance can help identify the likely degradation products, which can in turn help establish the degradation pathway and the intrinsic stability of the molecule. The degradation products usually arise from the ingredients used in dosage formulation and/or in the process of formulation where temperature, humidity and light may all play a part. To accelerate drug development, various stress-testing protocols had been designed to emulate stresses the compound may experience during manufacturing and storage conditions. These methods expose the drug to forced degradation conditions such as acid, base, oxidation and exposure to light. The Veterinary International Conference on Harmonization (VICH) guideline requires that stress testing be carried out to elucidate the stability characteristics of veterinary drug substance and medicinal products [2]. Information on the stability of the drug substance is an integral part of the systematic approach to stability evaluation.

Olaquindox, *N*-(2-hydroxyethyl)-3-methyl-2-quinoxalincarboxamide-1,4-dioxide, is one of the quinoxaline-*N*,*N*-dioxides that is used as medicinal feed additives for the prevention of pig dysentery and bacterial enteritis. Olaquindox is often responsible for induced photoallergic contact dermatitis and persistent light reaction in a pig breeder [3,4]. Detailed investigation of the identification of the photolysis products of this drug has not yet been carried on. The degradation behaviors of olaquindox in manure and environmentally relevant matrices, such as soil water and sewage sludge water, have been investigated, but the degradation products remain to identification [5,6].

LC–MS/MS has become the technique of choice in the degradation product studies due to its selectivity, sensitivity, and speed of analysis [7–9]. There have been a number of reports in the literature that applied LC–MS/MS for characterization of degradation products. In 2000, Wu [10] reviewed the application of LC–MS/MS in the analysis of drug degradation products in pharmaceutical formulations under various stress conditions (oxidation,

* Corresponding author. Tel.: +86 731 84635229; fax: +86 731 84673618.
E-mail address: sunzhiliang1965@yahoo.com.cn (Z.-L. Sun).

1387-3806/$ – see front matter © 2011 Elsevier B.V. All rights reserved.
doi:10.1016/j.ijms.2011.01.004

hydrolysis, dimerization and adduct formation with excipients). Exact mass measurements and elemental composition assignment are essential for the characterization of small molecules. Accurate mass measurement of the product ions facilitates the structural elucidation of new or unknown compounds [11]. Currently, liquid chromatography combined with hybrid ion trap/time-of-flight mass spectrometry (LC/MS-IT-TOF) provides high sensitivity and accuracy of the TOF analyzer with over 10,000 resolving power at m/z 1000. Moreover, multiple scans of metabolites in MS and MS^2 modes and accurate mass measurements can be automatically performed simultaneously through data-dependent acquisition. Although LC/MS-IT-TOF has rapidly developed as one of the most effective techniques for the determination of unknown compounds, its application to drug degradation product characterization is much less routine than for the drug metabolite characterization [12–14].

Therefore, the purpose of the present study was to perform stress studies on olaquindox in order to evaluate its inherent stability. To achieve this goal, we developed an LC/MS-IT-TOF method to characterize the degradation products of olaquindox in solutions. On the basis of accurate MS^2 spectra and elemental compositions of degradation products, we proposed their chemical structures. This work demonstrates that the use of LC/MS-IT-TOF approach appears to be rapid, efficient and reliable in structural characterization of degradation products.

2. Experimental

2.1. Chemicals

Olaquindox (99.8%) was obtained from China Institute of Veterinary Drug Control (Beijing, China). The stock solution of olaquindox was prepared by dissolving the compound in water at the concentration of 200 mg L^{-1}. HPLC-grade acetonitrile was purchased from Fisher Chemicals Co. (NJ, USA). Water was freshly prepared with the Millipore water purification system (MA, USA). All other chemicals and reagents were of the highest analytical grade available.

2.2. Stress studies

The stress studies were carried out under the conditions of hydrolysis, oxidation and photolysis. For all of the solution stability studies, the samples were prepared by mixing a dilute solution of olaquindox (200 mg L^{-1}) with various media (1:1; v/v). Acidic and alkaline hydrolysis were carried out in 0.1 N HCl and 0.1 N NaOH, respectively, whereas neutral hydrolysis was performed in water. All the hydrolytic studies were conducted at 80 °C for 12 h. The oxidative study was carried out in 30% H_2O_2 at room temperature for 12 h. The photostability testing was carried out by exposing the solution of drug in water to UV fluorescent light (208 W h/m^2) at room temperature for 12 h. All the stressed samples were withdrawn at suitable time intervals and diluted 10 times with water before injection into the LC/MS-IT-TOF.

2.3. LC/MS-IT-TOF analysis

For the characterization of olaquindox and its degradation products, hybrid IT/TOF mass spectrometry coupled with a high-performance liquid chromatography system was used (Shimadzu Corp., Kyoto, Japan). The liquid chromatography system (Shimadzu) was equipped with a solvent delivery pump (LC-20AD), an autosampler (SIL-20AC), a DGU-$20A_3$ degasser, a photodiode array detector (SPD-M20A), a communication base module (CBM-20A) and a column oven (CTO-20AC). The separation was performed on an ODS-C18 column (150 mm × 2.0 mm I.D.; particle size 5 μm) using a gradient elution consisting of mobile phase A (0.1% formic acid) and mobile phase B (acetonitrile). The gradient was as follows: 0–5 min, a linear gradient from 2% B to 5% B; 5–15 min, a linear gradient to 30% B; 15–18 min, a linear gradient to 100% B; 18–23 min, 100% B; 23–23.1 min, a linear gradient back to 2% B. The whole analysis took 25 min. The injection volume was 20 μL, the flow rate was 0.2 mL/min, and the PDA-detection was performed from 200 to 400 nm. The sample chamber in the autosampler was maintained at 4 °C, while the column was set at 40 °C.

The MS system consisted of a hybrid IT/TOF mass spectrometer (Shimadzu Corp., Kyoto, Japan) equipped with an electrospray ionization source. The total effluent from the detector was transferred directly to the hybrid IT/TOF mass spectrometer without splitting. The mass spectrometer was operated in the positive mode. Mass spectroscopy analyses were carried out on full-scan MS with a mass range of 100–400 Da and data-dependent MS/MS acquisition on the suspected precursor ions. Liquid nitrogen was used as the nebulizing gas at a flow rate of 1.5 L min^{-1}. The capillary and skimmer voltages were set at 4.5 kV and 1.6 kV, respectively. The CDL and heat block temperatures were both maintained at 200 °C. The MS^2 spectra were produced using CID of the selected precursor ions using argon as collision gas with relative energy of 50%. The ion accumulation time was set at 50 ms, the precursor ion isolation width at 1 Th. External mass calibration was carried out prior to data acquisition using direct infusion of a reference standard from 50 to 1000 Da. The reference standard was consisted of 0.25 mL L^{-1} trifluoroacetic acid and 0.1 g L^{-1} sodium hydrate. The flow rate of the infusion pump was 5 μL min^{-1}. All calculated mass error was less than 5 ppm after mass calibration with the reference standard.

Data acquisition and processing were carried out using the LC/MS solution version 3.41 software supplied with the instrument. Any mass numbers corresponding to particular elemental compositions were also calculated by the formula predictor, and would generate more than one formula proposed by the software. Therefore, an accuracy error threshold of ±20 ppm was set as a limit to the calculation of possible elemental compositions. The other following conditions for calculating elemental compositions were taken into consideration: the upper limits on the number of C, H, O, N, F atoms, C/H ratios, nitrogen rule and range of double-bond-equivalent (DBE).

3. Results and discussion

3.1. Degradation behaviors of olaquindox

The forced degradation samples of olaquindox (neutral, acidic, basic, oxidative and photolytic) were analyzed by LC/MS-IT-TOF to identify the degradation products. The representative HPLC chromatograms of olaquindox at each of the above stress conditions are shown in Fig. 1. Compared with the control (Fig. 1A), several peaks appeared in the chromatograms of the stressed samples (Fig. 1B–F). It indicated that olaquindox underwent degradation, and the highest concentration of degradation products was found in the acid-stressed sample (Fig. 1C). After 12 h exposure to the hydrolytic medias (neutral, acidic and basic) at 80 °C, nine, ten and four degradation products were formed under the neutral, acidic, basic conditions, respectively. However, four and seven degradation products were formed under the oxidative and photolytic conditions, respectively.

We assumed that they were degradation products of olaquindox because of comparison of the incubation sample with the standard solution, as well as the agreement between the accurate mass measurement in MS spectra and predicted formula calculation within 10 ppm. The predicted elemental compositions, measured accurate masses and exact masses, the mass errors, and the major fragment ions of the degradation products are indicated in Table 1. The exact

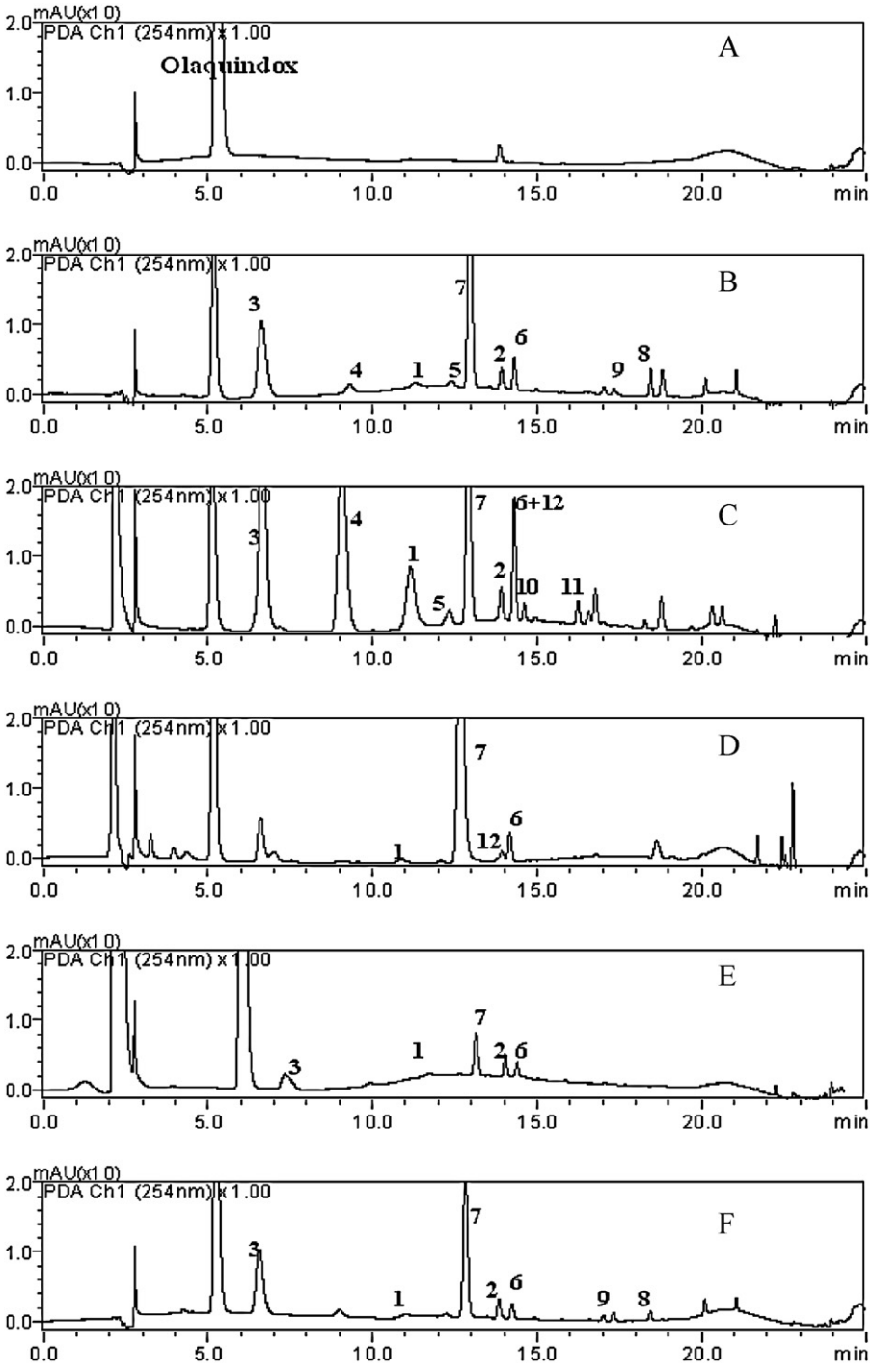

Fig. 1. LC–UV chromatograms of olaquindox standard solution (A), and the stressed olaquindox by H_2O for 12 h (B); 0.1 N HCl for 12 h (C); 0.1 N NaOH for 24 h (D); 30% H_2O_2 for 12 h (E); as well as UV fluorescent light at room temperature for 12 h (F).

and measured masses agree to within less than 10 ppm, providing support for the proposed elemental compositions of the degradation products. The accurate extracted mass chromatograms of the degradation products of olaquindox under various conditions are shown in Fig. 2.

3.2. Structural characterization of degradation products

Identification of degradation products was performed by hybrid ion trap/time-of-flight mass spectrometer that allows collision induced dissociation and accurate mass measurements on both fragment ions and precursors. This enables the user to determine the empirical formula for the unknown degradation products. The initial step in elucidating structures of degradation products of olaquindox is to understand the fragmentation pattern of the drug substance. The detailed mass spectrometry analysis of the fragmentation pattern of olaquindox provides a basis for assessing structural assignment for the degradation products. The detailed fragmentation pattern of olaquindox was reported in previous publication [12,15]. In this study, the comparison of the fragmentation pattern of the degradation products with that of olaquindox assigned the location of the medication. Mass accuracy measurements allowed the assignment of the molecular formula of fragment ions.

Table 1
The retention times (RT), measured accurate masses, predicated elemental compositions, theoretical masses, double bond equivalents (DBE), mass errors and major fragment ions of degradation products of olaquindox.

Degradation products	RT (min)	Measured mass (Da)	Elemental compositions ($[M+H]^+$)	DBE	Theoretical mass (Da)	Error (ppm)	Major fragment ion
Olaquindox	5.5	264.0971	$C_{12}H_{14}N_3O_4^+$	8	264.0979	−3.03	264.0840, 229.0793, 221.0534, 212.0791, 160.0612
1	11.6	248.1025	$C_{12}H_{14}N_3O_3^+$	8	248.1030	−2.02	230.0898, 161.0679, 143.0599
2	13.6	248.1026	$C_{12}H_{14}N_3O_3^+$	8	248.1030	−1.61	230.0898, 213.0896, 205.0607
3	7.5	264.0969	$C_{12}H_{14}N_3O_4^+$	8	264.0979	−3.79	246.0829, 177.0629, 160.0610
4	10.1	264.0961	$C_{12}H_{14}N_3O_4^+$	8	264.0979	−6.82	246.0816, 221.0561, 177.0634, 160.0583
5	12.6	266.1118	$C_{12}H_{16}N_3O_4^+$	8	266.1135	−6.39	206.0700
6	14.4	282.1065	$C_{12}H_{16}N_3O_5^+$	7	282.1084	−6.74	177.0646, 135.0533
7	13.1	177.0649	$C_9H_9N_2O_2^+$	7	177.0659	−5.65	160.0608, 132.0652
8	18.3	177.0651	$C_9H_9N_2O_2^+$	7	177.0659	−4.25	135.0515
9	17.5	222.0858	$C_{10}H_{12}N_3O_3^+$	7	222.0873	−6.75	135.0523
10	14.6	248.1025	$C_{12}H_{14}N_3O_3^+$	8	248.1030	−2.02	187.0486, 1161.0676, 159.0529
11	16.4	161.0693	$C_9H_{93}N_2O^+$	7	161.0709	−9.93	133.0740
12	14.1	193.0591	$C_9H_9N_2O_3^+$	8	193.0608	−8.81	176.0559, 159.0515, 148.0544

*3.2.1. Compounds **1** and **2***

Compounds **1** and **2** were eluted at retention times of 11.6 and 13.6 min, respectively. Both compounds showed a protonated molecule at *m/z* 248 and a loss of 16 Da (*m/z* 264–248) compared with olaquindox, suggesting that they were reduced degradation products of olaquindox. The difference between compounds **1** and **2** lay in the position of the N → O group reduction. Based on the accurate MS/MS spectra and in comparison to a previous report [12], compounds **1** and **2** were identified as 4-desoxyolaquindox and 1-desoxyolaquindox, respectively.

*3.2.2. Compounds **3** and **4***

Compounds **3** and **4** were eluted at retention times of 7.5 min and 10.1 min, respectively. Both compounds showed a protonated molecule at *m/z* 264, 16 Da higher than that of *m/z* 248, suggesting that they were oxidation product of compounds **1** or **2**. The compound eluting at 5.5 min possessed the same retention time, protonated molecule ion (*m/z* 264) and MS^2 spectrum as authentic olaquindox. Therefore, it was identified as unchanged olaquindox.

The MS^2 spectrum of compound **3** showed fragment ions at *m/z* 246 and 177 which are all 16 Da higher than fragment ions at *m/z* 230 and 161 of compound **1**, respectively, indicating that an oxygen atom had occurred on the quinoxaline ring. However, The MS^2 spectrum of compound **4** showed fragment ions at *m/z* 246 and 221 were all 16 Da higher than fragment ions at *m/z* 230 and 205 of compound **2**, respectively, indicating that it was an oxidation product of compound **2**. The presences of ions at *m/z* 177 and 160 of compounds **3** and **4** showed that the oxygen was located on the quinoxlaline ring. Considering the chemical structure of olaquindox and the oxidation environment, we proposed the oxygen atom had occurred on the methyl group of quinoxaline ring. Therefore, compounds **3** and **4** were identified as 3-hydroxymethyl-4-desoxyolaquindox and 3-hydroxymethyl-1-desoxyolaquindox, respectively.

*3.2.3. Compound **5***

Compound **5** was eluted at a retention time of 12.6 min and had a measured elemental composition of $C_{12}H_{16}N_3O_4$ ($[M+H]^+$ ion at *m/z* 266). Compound **5** had 2 Da higher than that of olaquindox, suggested that they were the hydrogenation product. The elemental composition of the fragment ion at *m/z* 206.0700 was $C_{10}H_{10}N_2O_3$ (predicted 206.0686 Da), according to the formula predictor software, indicating that C_2H_6NO was lost from *m/z* 266 to form *m/z* 206. This indicated the two hydrogen atoms of compound **5** were located on the N → O group to form N-hydroxyl.

*3.2.4. Compound **6***

Compound **6** was eluted at a retention time of 14.4 min and had a measured elemental composition of $C_{12}H_{16}N_3O_5$ ($[M+H]^+$ ion at *m/z* 282). Compound **6** had 18 Da higher than that of olaquindox, suggested that they were the oxidized products via the addition of a water molecule. The elemental compositions of the fragment ions at *m/z* 177.0646 and 135.0533 were $C_9H_9N_2O_2$ (predicted 177.0659 Da) and $C_7H_7N_2O$ (predicted 135.0553 Da), respectively, according to the formula predictor software, indicating that C_2H_2O was lost from *m/z* 177 to form *m/z* 135. This indicated the oxygen atom of compound **6** was located on the methyl group of quinoxaline ring.

*3.2.5. Compounds **7** and **8***

Compounds **7** and **8** were eluted at the retention times of 13.1 and 18.3 min, respectively. Both compounds showed similar protonated molecule at *m/z* 177.0649 and *m/z* 177.0651 and the same predicated elemental composition of $C_9H_9N_2O_2$. Compound **7** fragmented to yield abundant product ion at *m/z* 160 corresponding to the loss of OH radical from *m/z* 177, suggesting an N → O group of compound **7** was existed on the quinoxaline ring. The loss of CO from the ion *m/z* 160 leaded to fragment ion at *m/z* 132, which indicated the presence of phenol within this molecule. In addition, the N → O group reduction at position 1 is relatively easy with respect to the electronic effect, because reduction of the N → O group at position 4 is hindered by the adjacent methyl group. Therefore, compound **7** was identified as 3-methyl-2-hydroxylquinoxaline-4-oxide. However, the MS^2 spectrum of compound **8** showed fragment ion at *m/z* 135 was in accordance with that from compound **6**, indicating that oxygen atom had occurred on the methyl group of quinoxaline ring. Therefore, compound **8** was identified as 3-hydroxymethylquinoxaline-4-oxide.

*3.2.6. Compound **9***

Compound **9** was eluted at a retention time of 17.5 min and had a measured elemental composition of $C_{10}H_{12}N_3O_3$ ($[M+H]^+$ ion at *m/z* 222). The elemental composition of the fragment ion at *m/z* 135.0526 was $C_7H_7N_2O$ (predicted 135.0553 Da), according to the formula predictor software, indicating that $C_3H_5NO_2$ was lost from *m/z* 222 to form *m/z* 135. The MS^2 spectrum of compound **9** showed fragment ion at *m/z* 135 was in accordance with that from compound **6**, indicating that oxygen atom had occurred on the methyl group of quinoxaline ring. Therefore, compound **9** was identified as 3-hydroxymethyl-2-quinoxalinecarboxamide-4-oxide.

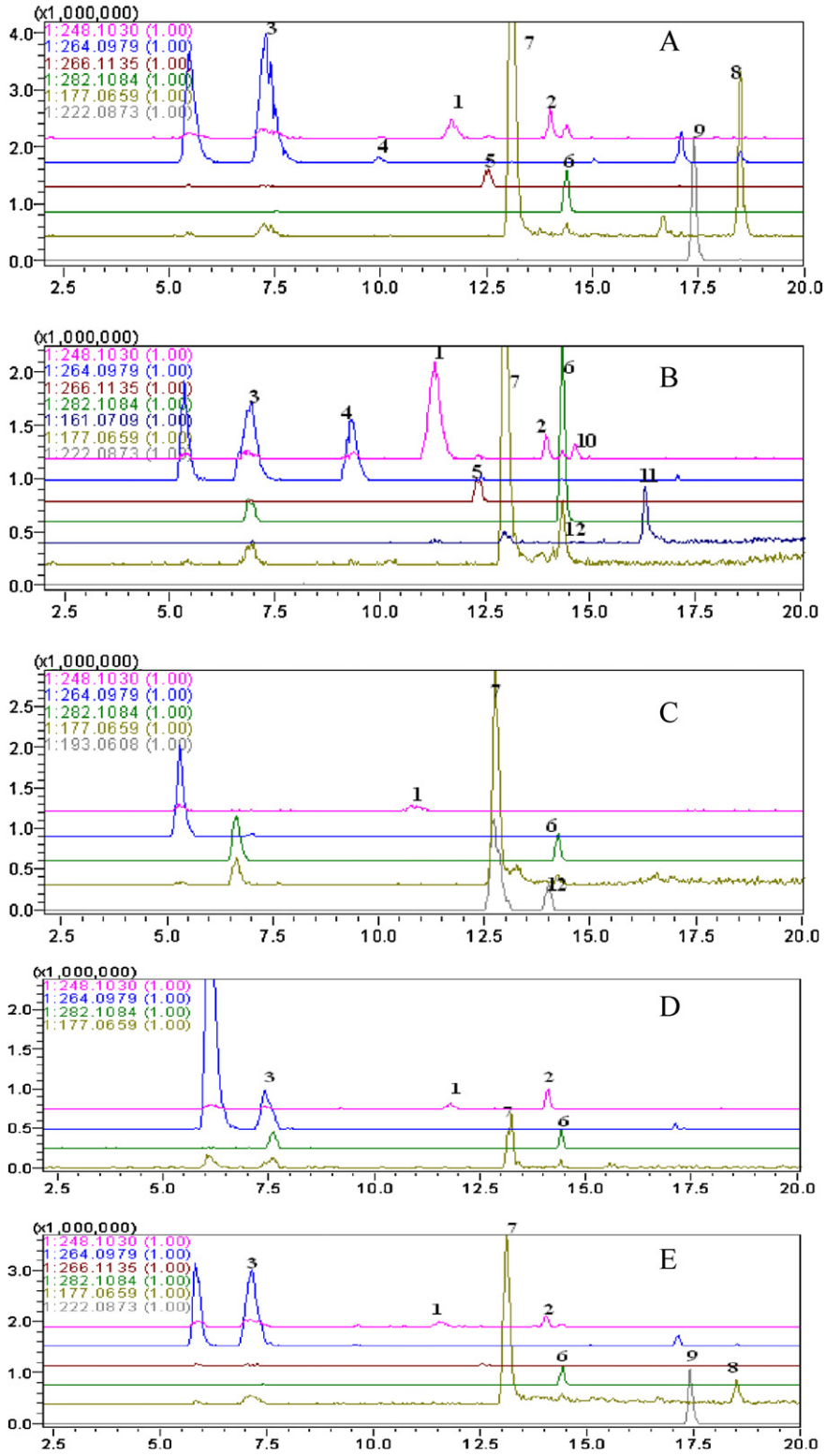

Fig. 2. The accurate extracted mass chromatogram (EIC) of degradation products of olaquindox under the stressed by H_2O for 12 h (A); 0.1 N HCl for 12 h (B); 0.1 N NaOH for 24 h (C); 30% H_2O_2 for 12 h (D); as well as UV fluorescent light at room temperature for 12 h (E).

3.2.7. Compound ***10***

Compound **10** was eluted at a retention time of 14.6 min and had a measured elemental composition of $C_{12}H_{14}N_3O_2$ ($[M+H]^+$ ion at *m*/*z* 248). Compound **10** had 16 Da lower than that of olaquindox, suggested that it was the reduced products of parent drug. No fragment ion at *m*/*z* 230 was observed in the MS^2 spectrum of compound **9**, indicating the side chain was vulnerable to cleavage to form the fragment ions at *m*/*z* 187 and 161. The elemental compositions of the fragment ions at *m*/*z* 187.0486 and 159.0529 were $C_{10}H_7N_2O_2$ (predicted 187.0502 Da) and $C_9H_7N_2O$ (predicted 159.0513 Da), respectively, according to the formula predictor software, indicating that CO was lost from *m*/*z* 187 to form *m*/*z* 159. Therefore, the oxygen atom of compound **10** was located on the methyl group of quinoxaline ring.

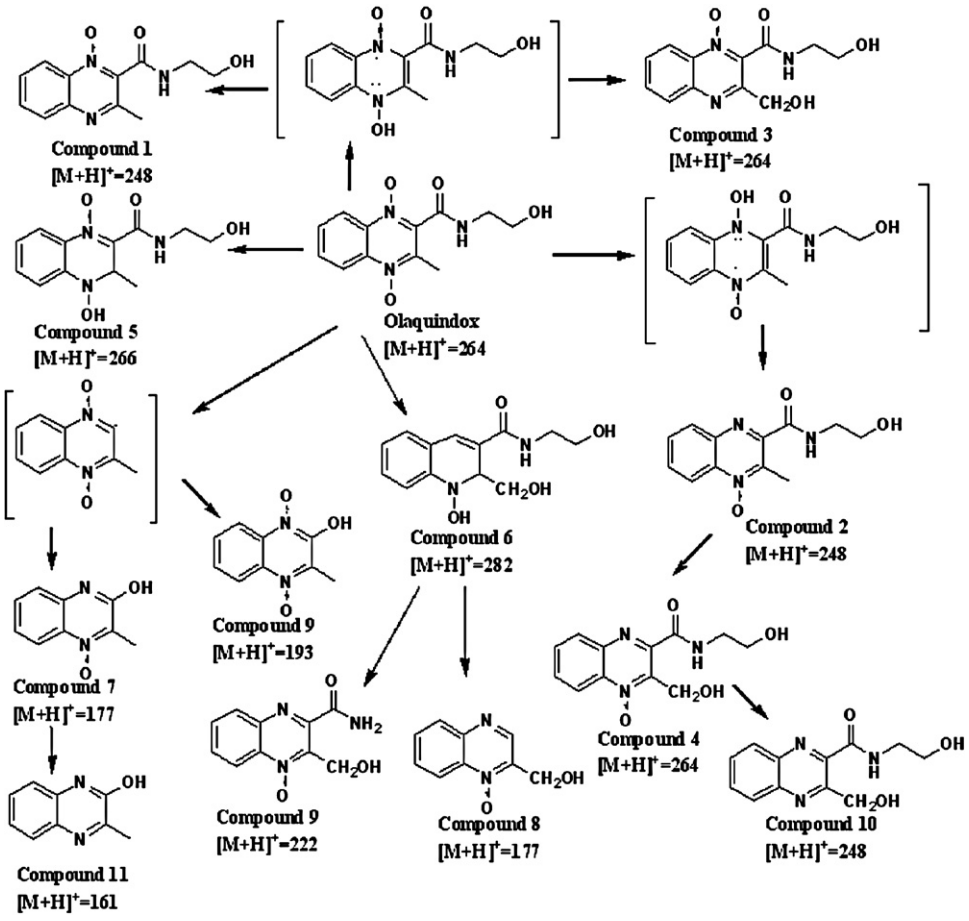

Fig. 3. The proposed degradation pathway of olaquindox.

*3.2.8. Compound **11***

Compound **11** was eluted at a retention time of 16.4 min and had a measured elemental composition of $C_9H_9N_2O$ ($[M+H]^+$ ion at *m*/*z* 161). It fragments to yield product ion at *m*/*z* 133 corresponding to the loss of CO from *m*/*z* 161, suggesting that the presence of phenol within this molecule. Therefore, compound **11** was identified as 3-methyl-2-hydroxylquinoxaline.

*3.2.9. Compound **12***

Compound **12** was eluted at a retention time of 14.1 min and had a measured elemental composition of $C_9H_8N_2O_3$ ($[M+H]^+$ ion at *m*/*z* 193). The fragment ion at *m*/*z* 176 indicated the loss of an OH radical from *m*/*z* 193, and a further loss of OH to form the fragment ion at *m*/*z* 159, indicating the two N → O group were existed on the compound **12**. The MS^2 spectrum of compound **12** showed fragment ions at *m*/*z* 176 and 148 were all 16 Da higher than fragment ions at *m*/*z* 160 and 132 of compound **7**, respectively. Therefore, compound **12** was identified as 3-methyl-2-hydroxylquinoxaline-1,4-dioxide.

3.3. Degradation pathways of olaquindox

Under various conditions, N → O group of olaquindox was reduced to form the compounds **1** and **2** via the N-oxide radical intermediate according to a mechanism proposed by Inbaraj et al. [16]. The hydroxyl radical was also produced during the formation of compounds **1** and **2**. Thus, the phototoxicity and the photoallergic reaction of the drug could be explained by the formation of a radical intermediate and hydroxyl radical that could readily react with DNA. The N-oxide radicals could undergo further oxidation leading to the generation of hydroxylation compounds. The oxidation of the N-oxides in soil has already been described for quinoxaline N-oxides by Zhang and Huang [17]. Olaquindox also readily underwent cleavage of side chain under hydrolytic and photolytic conditions to form compounds **7** and **12**. The cleavage of side chain of quinoxaline might accord with the mechanism proposed for other drugs such as ciprofloxacin [18]. Based on these results, the schematic representation of the degradation pathways is tentatively proposed as shown in Fig. 3.

4. Conclusion

In the present study, we demonstrated the application of liquid chromatography combined with hybrid ion trap/time-of-flight mass spectrometry for the detection and structural characterization of degradation products of olaquindox. The chromatographic method we described here can resolve almost degradation products from the parent as well as from each other under various different conditions. Olaquindox underwent most degradation under the acidic conditions to 10 products. The degradation was mild under photolytic conditions, forming a total of seven products, but in small quantities. All degradation products were characterized with the help of the accurate mass measurements of fragment ions and precursors. A comprehensive degradation pathway of olaquindox was tentatively outlined. It was also found that N-oxide radical intermediates and hydroxyl radicals were formed during the degradation process. Hence, the study of degradation products of olaquindox may give insight onto the mechanisms leading to the phototoxicity and the photoallergic reaction of the drug.

Acknowledgment

This work is supported financially by Major Projects of Science and Technology of Hunan Province (2009FJ1005).

References

[1] K.M. Alsante, L. Martin, S.W. Baertschi, A stress testing benchmarking study, Pharm. Technol. 27 (2003) 60–72.
[2] VICH International Conference on Harmonisation of Technical requirements for registration of Veterinary Medicinal Products, Stability testing of new veterinary drug substance and medicinal products (1999) 1–19.
[3] F.G. Dunkel, P. Elsner, Y. Pevny, G. Burg, Olaquindox-induced photoallergic contact dermatitis and persistent light reaction in a pig breeder, Contact Dermat. 23 (1990) 283.
[4] A. Kumar, S. Freeman, Photoallergic contact dermatitis in a pig farmer caused by olaquindox, Contact Dermat. 35 (1996) 249–250.
[5] F. Ingerslev, B. Halling-Sorensen, Biodegradability of metronidazole, olaquindox, and tylsoin and formation of tylosin degradation products in aerobic soil-manure slurries, Ecotoxicol. Environ. Saf. 48 (2001) 311–320.
[6] B. Halling-Sorensen, G. Sengelov, F. Ingerslev, L.B. Jensen, Reduced antimicrobial potencies of oxytetracycline, tylosin, sulfadiazin, streptomycin, ciprofloxacin, and olaquindox due to environmental processes, Arch. Environ. Contam. Toxicol. 44 (2003) 7–16.
[7] W. Feng, H. Liu, G. Chen, R. Malchow, F. Bennett, E. Lin, B. Pramanik, T.M. Chan, Structural characterization of the oxidation degradation products of an antifungal agent SCH 56592 by LC–NMR and LC–MS, J. Pharm. Biomed. Anal. 25 (2001) 545–557.
[8] M.S. Lee, E.H. Kerns, LC/MS application in drug development, Mass Spectrom. Rev. 18 (1999) 187–279.
[9] K.J. Volk, E.S. Hill, E.H. Kerns, M.S. Lee, Profiling degradants of paclitaxel using liquid chromatography–mass spectrometry and liquid chromatography–tandem mass spectrometry substructural techniques, J. Chromatogr. B: Biomed. Sci. Appl. 696 (1997) 99–115.
[10] Y. Wu, The use of liquid chromatography–mass spectrometry for the identification of drug degradation products in pharmaceutical formulations, Biomed. Chromatogr. 14 (2000) 384–396.
[11] L.K. Zhang, B.N. Pramanik, Characterization of major degradation products of an adenosine A2A receptor antagonist under stressed conditions by LC–MS and FT tandem MS analysis, J. Mass. Spectrom. 45 (2010) 146–156.
[12] Z. Liu, L. Huang, M. Dai, D. Chen, Y. Wang, Y. Tao, Z. Yuan, Metabolism of olaquindox in rat liver microsomes: structural elucidation of metabolites by high-performance liquid chromatography combined with ion trap/time-of-flight mass spectrometry, Rapid Commun. Mass Spectrom. 22 (2008) 1009–1016.
[13] Z. Liu, L. Huang, M. Dai, D. Chen, Y. Tao, Y. Wang, Z. Yuan, Metabolism of cyadox in rat, chicken and pig liver microsomes and identification of metabolites by accurate mass measurements using electrospray ionization hybrid ion trap/time-of-flight mass spectrometry, Rapid Commun. Mass Spectrom. 23 (2009) 2026–2034.
[14] Z.Y. Liu, L.L. Huang, D.M. Chen, M.H. Dai, Y.F. Tao, Y.L. Wang, Z.H. Yuan, Application of electrospray ionization hybrid ion trap/time-of-flight mass spectrometry in the rapid characterization of quinocetone metabolites formed in vitro, Anal. Bioanal. Chem. 396 (2010) 1259–1271.
[15] X.S. Miao, R.E. March, C.D. Metcalfe, A tandem mass spectrometric study of the N-oxides, quinoline N-oxide, carbadox, and olaquindox, carried out at high mass accuracy using electrospray ionization, Int. J. Mass Spectrom. 230 (2003) 123–133.
[16] J.J. Inbaraj, A.G. Motten, C.F. Chignell, Photochemical and photobiological studies of tirapazamine (SR 4233) and related quinoxlaine 1,4-di-N-oxide anlaogues, Chem. Res. Toxicol. 16 (2003) 164–170.
[17] H. Zhang, C.H. Huang, Reactivity and transformation of antibacterial N-oxides in the presence of manganese oxide, Environ. Sci. Technol. 39 (2005) 593–601.
[18] T.G. Vasconcelos, D.M. Henriques, A. Konig, A.F. Martins, K. Kummerer, Photodegradation of the antimicrobial ciprofloxacin at high pH: identification and biodegradability assessment of the primary by-products, Chemosphere 76 (2009) 487–493.